Temperature dependence of the low frequency dynamics of myoglobin

Measurement of the vibrational frequency distribution by inelastic neutron scattering

Stephen Cusack* and Wolfgang Doster[‡]

*EMBL Grenoble Outstation, c/o ILL, 156X, 38042 Grenoble Cedex, France and [‡]Physik Department E13, Technische Universität München, D-8046 Garching, Federal Republic of Germany

ABSTRACT   Inelastic neutron scattering spectra of myoglobin hydrated to 0.33 g water (D_2O)/g protein have been measured in the low frequency range ($1-150$ cm^{-1}) at various temperatures between 100 and 350 K. The spectra at low temperatures show a well-resolved maximum in the incoherent dynamic structure factor $S_{inc}(q, \omega)$ at ~25 cm^{-1} and no elastic broadening. This maximum becomes gradually less distinct above 180 K due to the increasing amplitude of quasielastic scattering which extends out to 30 cm^{-1}. The vibrational frequency distribution derived independently at 100 and 180 K are very similar, suggesting harmonic behavior at these temperatures. This result has been used to separate the vibrational motion from the quasielastic motion at temperatures above 180 K. The form of the density of states of myoglobin is discussed in relation to that of other amorphous systems, to theoretical calculations of low frequency modes in proteins, and to previous observations by electron-spin relaxation of fractal-like spectral properties of proteins. The onset of quasielastic scattering above 180 K is indicative of a dynamic transition of the system and correlates with an anomalous increase in the atomic mean-squared displacements observed by Mössbauer spectroscopy (Parak, F., E. W. Knapp, and D. Kucheida. 1982. *J. Mol. Biol.* 161:177–194.) and inelastic neutron scattering (Doster, W., S. Cusack, and W. Petry. 1989. *Nature [Lond.].* 337:754–756.) Similar behavior is observed for a hydrated powder of lysozyme suggesting that the low frequency dynamics of globular proteins have common features.

1. INTRODUCTION

Mössbauer spectroscopy (1, 2) has demonstrated the existence of a striking transition in the dynamical behavior of myoglobin at ~200 K characterized by a marked increase with temperature of the mean squared displacement of the heme iron which is correlated with the onset of motions on the time scale of $10^{-7}–10^{-9}$ s. These observations have been interpreted on the basis of a model of protein dynamics originally proposed to explain the temperature dependence of ligand binding in myoglobin (3, 4). It is supposed that a folded protein can exist in multiple conformational substates corresponding to multiple minima in the potential energy surface of the protein. At physiological temperatures there can be rapid transitions between these substates whereas at low temperatures (typically below 200 K) there is the possibility that individual molecules become 'frozen' into different substates which may have different functional properties (e.g., different ligand rebinding rates). Further evidence for this picture has come from the x-ray structure analysis of myoglobin down to 80 K (5) and an analysis of a molecular dynamics simulation of myoglobin (6). It has also been shown that the transition in the mobility of myoglobin above 200 K correlates with a glass-like transition in the hydration water (7).

In this and a related paper (8) we demonstrate that the dynamic transition in myoglobin can also be observed using inelastic neutron scattering. Using this technique (9–12) motions faster than 10^{-10} s can be resolved and the markers of protein motion are the hydrogen atoms (due to the anomalously large incoherent neutron scattering cross-section of the ^1H nucleus) which are generally uniformly distributed throughout the protein. The quantity measured is the incoherent dynamic structure factor $S_{inc}(q, \omega)$ which is the space-time Fourier transform of the self-correlation function $G_s(r, t)$ which describes the correlation of the position of an atom at time 0 with the position of the *same* atom at time t.

We find that up to 180 K the dynamics of hydrated myoglobin are consistent with harmonic behavior, that is, the atomic mean-squared displacements increase linearly with temperature and only vibrational motion is apparent in the inelastic spectrum. There is a resolved maximum in the dynamic structure factor at ~25 cm^{-1}. Above 180 K we observe the onset of other dynamical processes which manifest themselves (analogously to Mössbauer spectroscopy) by the anomalous decrease in the Debye-Waller factor above 180 K corresponding to a marked increase in the mean-squared atomic displacements (8). This is accompanied by the appearance of a broad quasielastic line superimposed on the background vibrational motion which ultimately submerges the maximum at 25 cm^{-1} observed at low temperatures to give at higher tempera-

tures a spectrum monotonically decreasing with frequency.

In this paper we focus on the vibrational part of the spectrum of myoglobin. The vibrational frequency distribution, $G(\omega)$, of myoglobin is derived at temperatures between 100 and 350 K using a modification of the usual method of extrapolation of the incoherent scattering to $q = 0$ which takes into account multiple scattering. At low temperatures (below 200 K), where there is no quasi-elastic scattering, $G(\omega)$ is found to be Debye-like ($G[\omega] \propto \omega^2$) at very low frequencies followed by a cross-over to a weaker dependence on frequency above 25 cm^{-1}. The observed peak in the dynamic structure factor at 25 cm^{-1} manifests itself as an enhancement in the density of states. The results for higher temperatures show that it is a good approximation to assume that the vibrational motion remains essentially harmonic above 200 K. This allows the quasielastic spectrum to be separated above 200 K and this has been further analyzed in a previous paper (8).

The features in the density of states reported here are reminiscent of those found in other amorphous systems and glasses and are also predicted for systems with fractal geometry. The results for myoglobin are therefore discussed in relation to various theories of low frequency vibrations in amorphous systems and also to earlier low-frequency Raman spectroscopy and electron spin-relaxation results on proteins. Furthermore the neutron scattering measurements reported here cover exactly the same picosecond time domain that is currently accessible to molecular dynamics simulations of proteins or other models of protein dynamics such as normal mode analysis. It is therefore important to try and compare these experimental results with detailed theoretical calculations to assess the reliability of the empirical potential energy functions used in the latter. This has been done recently with regard to the frequency distribution of bovine pancreatic trypsin inhibitor (BPTI; 13, 14).

2. METHODS

Measurements were made on the time focusing time-of-flight spectrometer IN6 at the Institut Laue-Langevin (ILL), Grenoble, France (15). The spectrometer was operated with a wavelength of 5.1 Å and the detectors grouped to give 19 spectra at scattering angles between 13° and 114° (corresponding to elastic q between 0.27 and 2.05 Å $^{-1}$). The accessible energy range is 1–500 cm^{-1}. The energy resolution function of this instrument is closely Gaussian with sigma measured at the elastic peak increasing from 0.24 cm^{-1} at low angles to 0.48 cm^{-1} at high angles. The resolution deteriorates rapidly with increasing energy shift. Spectra were accumulated for 3–8 h. Initial data reduction was performed using standard ILL programs which correct for incident flux, cell scattering, and self-shielding (using angle dependent slab corrections (12) and measured transmissions) and detector response (using a

vanadium spectrum as a standard). The resultant spectra, put on an absolute scale, are the basis of the discussion in this paper.

Samples for IN6 were measured in a thin walled, vacuum tight aluminium cell of diam 50 mm and interwall spacing 1.5 mm with the sample at 135° to the incident beam. Hydrated samples of sperm whale myoglobin were obtained by rehydration of lyophilized material (Sigma Chemical Co., St. Louis, MO) with D_2O (0.33 g D_2O/g protein) in a controlled humidity environment (provided by D_2O saturated with potassium nitrate). Under these hydration conditions, the incoherent scattering from the unexchanged ^1H atoms of the protein ($-CH$, $-CH_2$, $-CH_3$, and some very slowly exchanging $-NH$) contribute more than 98% of the total sample incoherent scattering. Typically 300–500 mg of sample were used giving neutron transmissions of 92–86%. Temperature was easily variable between 100 and 350 K (with stability 0.5 degrees) by means of a computer controlled heater/cold nitrogen gas flow. The structure of the D_2O-hydrated sample of myoglobin used for the inelastic measurements is currently being characterized by neutron small-angle scattering using the instrument D16 at the Institut Laue-Langevin.

The amplitude-weighted frequency distribution $G(\omega)$ was obtained from the time-of-flight spectra at different angles by a novel procedure which takes into account multiple scattering (Cusack, S., unpublished results). $G(\omega)$ is defined for a spherically averaged system by the limit:

$$G(\omega) = \lim_{q \to 0} \frac{6\omega}{\hbar q^2} (e^{\hbar\omega/k_BT} - 1) S_{inc}(q, \omega)$$

$$= \sum_{\lambda=1}^{3N-6} \sum_{L=1}^{N} \frac{\sigma_L^{inc}}{4\pi m_L} |c_L^\lambda|^2 \delta(\omega - \omega_\lambda), \quad (1)$$

where the second term corresponds to the result for a harmonic system of N atoms with normal modes of frequency ω_λ and eigenvectors c_L^λ and incoherent neutron cross-section σ_L^{inc}. This is based on the dominance as $q \to 0$ of the one-phonon contribution to $S_{inc}(q, \omega)$:

$$S_{inc}(q, \pm\omega_\lambda)$$

$$= e^{\pm\hbar\omega_\lambda/k_BT} \sum_{L=1}^{N} \frac{\sigma_L^{inc}}{4\pi} e^{-2W_L(q)} \frac{\hbar |q \cdot c_L^\lambda|^2}{4\omega_\lambda m_L \sinh(\hbar\omega_\lambda/2k_BT)}, \quad (2)$$

where $W_L(q)$ is the Debye-Waller exponent for atom L. It will now be assumed that for powder samples of very complex polyatomic molecules as studied here, anisotropic effects in Eq. 2 (e.g., due to the normal mode eigenvectors) and the complications arising from the many inequivalent atoms, can be ignored and the resultant spherically averaged incoherent structure factor can be expressed in terms of an isotropic amplitude-weighted frequency distribution $G(\omega)$ and frequency-dependent Debye-Waller factor exponent $q^2U(\omega)$. ($U[\omega]$ can be thought of as an average mean-square displacement). The justification of this is empirical (see below) and also discussed elsewhere with reference to a calculated normal mode model of BPTI, a small protein (16). There it is shown that the amplitude-weighted frequency distribution that would be measured by incoherent neutron scattering has very closely the same form as the true normal mode frequency distribution $g(\omega)$. This is due to the good sampling of the motion in different parts of the protein by the uniformly distributed hydrogen atoms.

In practice the experimental data were found to conform very well to the empirical equation:

$$S(q, \omega) = \frac{\hbar q^2}{6\omega} \frac{1}{(e^{\hbar\omega/k_BT} - 1)} G(\omega) e^{-q^2U(\omega)} + M(\omega), \quad (3)$$

where $M(\omega)$ is a small but significant angle-independent (i.e., q-independent) term (see dashed curve in Fig. 3 b). Subsequently it has been shown that the term $M(\omega)$ can be accounted for quantitatively using the multiple scattering theory of Sears (17) (see also reference 12 for a discussion of multiple scattering). $M(\omega)$ arises from double scattering of the form elastic-inelastic and can be significant because of the extremely intense elastic peak (and correspondingly weak inelastic scattering) from the samples measured. As long as the elastic intensity varies only slowly with q i.e., $S(q, 0) \sim S(0)$, this double scattering can be shown (Cusack, S., unpublished results) to be approximately given by the expression $M(\omega) \sim \Delta S(q_0, \omega) S(0)$, where Δ is a constant depending on the sample cross-section (defined by Eq. [6.2.8] in reference 17), and $q_0 = q_0(\omega)$ is the scattering vector for 90° scattering. Thus $M(\omega)$ is expected to be essentially angle-independent and of the same form as the single inelastic scattering, as observed (*dashed curve*, Fig. 3 b). Good quantitative agreement is found for its observed magnitude and that predicted by the theory for the slab geometry and sample transmission used in the experiment. (Cusack, S., unpublished results).

The ensemble of time-of-flight data can thus be reduced in principal to three frequency-dependent functions $G(\omega)$, $U(\omega)$, and $M(\omega)$ by least squares fitting Eq. 3 to the 18 different q-values measured at each frequency. In practice, the limited range of q of the data do not allow the Debye-Waller factor to be independently defined as it is strongly correlated with $G(\omega)$ (i.e., the same value of $S[q, \omega]$ can be obtained by increasing both $G[\omega]$ and $U[\omega]$). This problem was overcome by using a fixed (frequency independent) Debye-Waller factor, $\exp[q^2 U_{vib}(T)]$, for each temperature, with $U_{vib}(T)$ being determined from examination of ratio plots as defined by Eq. 6 and shown in Fig. 2. The solid lines in Fig. 2 are the ratios (right hand side of Eq. 2) expected for a system showing purely harmonic behavior and depend only on the Bose occupation factors. Agreement between theory and the measured data is very good above 30–40 cm^{-1} for a particular choice of Debye-Waller factor, namely with $U_{vib}(T) = 0.0001 \times T(K)$ Å^2 ($T > 100$ K), where we have assumed a linear temperature dependence as appropriate to a harmonic system. This temperature dependence of the vibrational Debye-Waller factor is very close to that derived from an independent analysis (8) of the elastic peak intensity as a function of q and T; this analysis gave $U_{vib}(T) = 0.00016 \times (T - 50)$ Å^2 ($T > 100$). Although this method of determination of the Debye-Waller factor is rather sensitive, remaining uncertainty in its value does lead to a corresponding uncertainty in the magnitude of the derived $G(\omega)$ at each temperature. For example, $U_{vib}(T)$ at $T = 250$ K has been taken as 0.025 Å^2; if the value were really as much as 0.04 Å^2 (an error bigger than estimated), for a typical value of $q = 2.5$ Å^{-1}, the Debye-Waller factor would be smaller by $\exp[-2.5^2 \times (0.04 - 0.025)] = 0.91$. Thus, the derived $G(\omega)$ would be about 10% larger. However, the form of the density of states is much less sensitive to the Debye-Waller factor as the frequency dependent effects are only slowly varying. In particular the conclusions in section 4b and 4c are not affected.

In reference 16 there is a fuller discussion of attempts to simplify Eq. 2 while preserving the effects of inequivalent atoms (i.e., with different Debye-Waller factors) and multiphonon scattering. However, the expressions derived contain more parameters than in Eq. 3, and the apparent information content of the current data does not justify their use.

3. RESULTS

Fig. 1 shows the incoherent structure factor of D$_2$O-hydrated myoglobin for a fixed scattering angle (108°) for temperatures between 100 and 350 K. These spectra are simply a transformation of the original time-of-flight

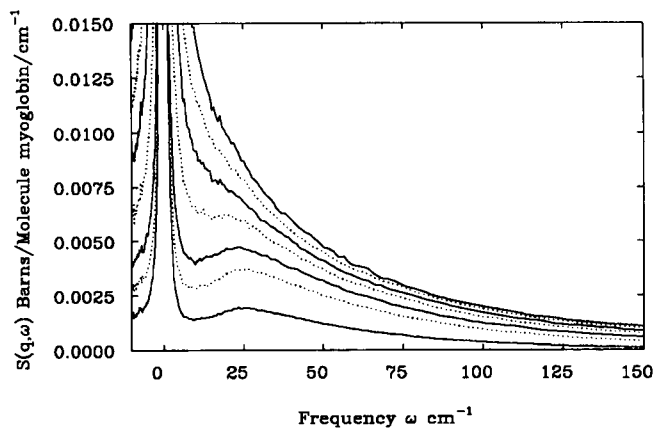FIGURE 1   The temperature dependence of $S(q, \omega)$ for D$_2$O-hydrated myoglobin for a mean scattering angle of 108.3°. The temperatures are 100 K (*bottom curve*), 180 K, 220 K, 270 K, 300 K, 320 K, and 350 K (*top curve*). The data are on an absolute scale (with accuracy $\sim$10%), as determined by a vanadium standard.

spectra. The spectra at 100 and 180 K show no broadening of the elastic line and a well-resolved maximum at 25 cm^{-1}. Above 180 K this maximum becomes less and less distinct due to the increasing intensity of a broad quasielastic line.

We first show that we can analyze these data by separating contributions from elastic, quasielastic, and inelastic scattering according to the expression (12).

$$S(q, \omega, T) = e^{-q^2 U_{vib}(T)}$$
$$\cdot [A(q, T)\delta(\omega) + S_{qel}(q, \omega, T) + S_{vib}(q, \omega, T)], \quad (4)$$

where $A(q, T)$ is the elastic incoherent structure factor, the quasielastic scattering is given by $S_{qel}(q, \omega, T) = [1 - A(q, T)]S'_{qel}(q, \omega, T)$, where $S'_{qel}(q, \omega, T)$ is normalized to unity over frequency and

$$S_{vib}(q, \omega, T) \approx \frac{\hbar q^2}{6\omega(e^{\hbar\omega/k_B T} - 1)} G(\omega) \quad (5)$$

is the one-phonon vibrational scattering, with $q^2 U_{vib}(T)$ as the vibrational Debye-Waller factor exponent. Eq. 4 is understood to be convoluted with the instrumental resolution function.

In Eqs. 4 and 5 we have assumed that the vibrational frequency distribution $G(\omega)$ is temperature independent and that the temperature dependence of the vibrational scattering occurs only in the Debye-Waller and Bose factors as in a harmonic system. That this is a good approximation can be seen from ratio plots as previously used by Frick et al. in their study of the glass transition in polybutadiene (18). Outside the frequency range of the

quasielastic scattering we should find:

$$\frac{S(q, \omega, T)}{S(q, \omega, T_0)} \frac{e^{-q^2 U_{vib}(T_0)}}{e^{-q^2 U_{vib}(T)}}$$

$$= \frac{(e^{\hbar\omega/k_B T_0} - 1)}{(e^{\hbar\omega/k_B T} - 1)} \approx \frac{T}{T_0}\left[1 + \frac{\hbar\omega}{2k_B}\left(\frac{1}{T_0} - \frac{1}{T}\right)\right], \quad (6)$$

where T_0 is a reference temperature where the quasielastic scattering is zero. Fig. 2 shows such ratios for $T_0 = 180$ K. These demonstrate that the quasielastic scattering falls to zero beyond ~ 4 meV (32 cm^{-1}) and that above this frequency the inelastic scattering is to a very good approximation taken into acount by the quasiharmonic temperature scaling. In evaluating Eq. 6 we have taken $U_{vib}(T) = 0.0001 \times T(K)$ Å^2; much less good agreement is obtained with $U_{vib}(T)$ differing by more than 20%. Indeed we have used these ratios as a rather sensitive method of determining the Debye-Waller factor (see end of section 2). In section 4d we show how the quasielastic contribution can be obtained by subtracting the inelastic part.

The data at each temperature have been used to derive independently the frequency distribution $G(\omega)$ according to the method described above with a fixed Debye-Waller factor for each temperature. As an example of the fitting procedure, Fig. 3 a shows the unsmoothed spectra at 180 K for nine of the eighteen scattering angles between 17° and 112° and Fig. 3 b shows the same data (*dots*) with superimposed solid curves recalculated using the two fitted functions $G(\omega)$, $M(\omega)$, and $U(\omega) = U_{vib}$ according to Eq. 3. Also shown is the angle-independent function $M(\omega)$ which arises from multiple scattering. The good quality of the fits demonstrates that the data are well explained by Eq. 3. Fig. 4 shows the frequency distribution $G(\omega)$ at 100 K, 180 K, 250 K, 300 K, and 350 K
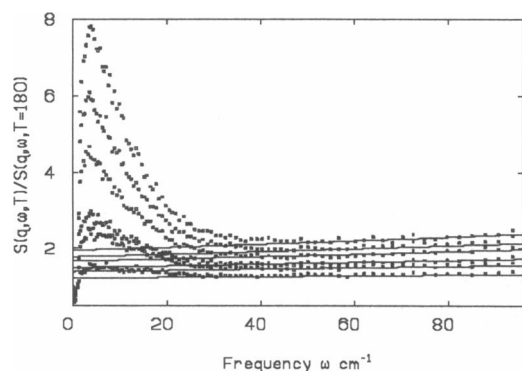

FIGURE 3 (a) $S(q, \omega)$ for D$_2$O-hydrated myoglobin at 180 K for a series of scattering angles: 16.8 (*bottom curve*), 25.9, 35.4, 50.6, 61.2, 71.8, 84.6, 97.3, 111.6° (*top curve*). (b). The same data (*dots*) as in a plotted with curves recalculated from the fitted functions $G(\omega)$, $M(\omega)$, and U_{vib} (*solid lines*). The angle-independent multiple scattering contribution $M(\omega)$ is shown dashed.

FIGURE 2 Ratios $S(q, \omega, T)/S(q, \omega, T_0 = 180)$ at a fixed scattering angle of 108.3°. The solid lines give the Bose-factor ratios (right hand side of Eq. 6). The temperatures are 220 K (*bottom curve*), 250 K, 270 K, 300 K, 320 K, and 350 K (*top curve*).
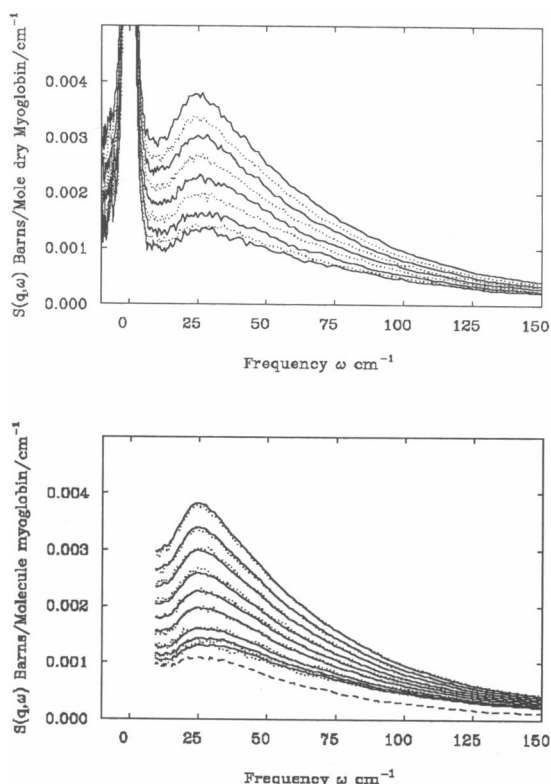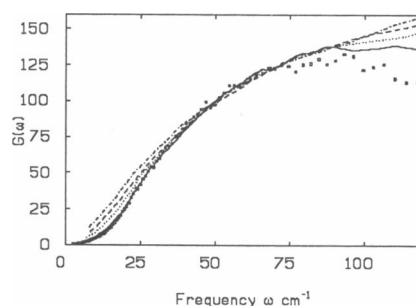

FIGURE 4 The amplitude-weighted vibrational frequency distribution $G(\omega)$ of D$_2$O-hydrated myoglobin derived independently at 100 K (*small circles*) and 180 K (*solid*), 250 K (*dots*), 300 K (*dash*), and 350 K (*dotdash*). The 100 K curve has been scaled by a constant factor 1.04 to bring it into near superposition with the 180 K curve. This difference could be accounted for by errors in transmission measurements. The statistical errors calculated from the fitting routine at each energy are between 2 and 4% for all curves.
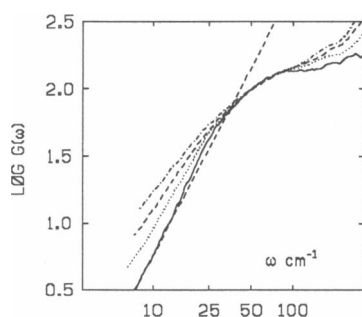
FIGURE 5 Log/log plot of the amplitude-weighted vibrational frequency distribution of myoglobin at 180 K (*solid*), 250 K (*dots*), 300 K (*dash*), and 350 K (*dotdash*). The dashed straight line has slope 2 (Debye behavior).

(note that the quasielastic scattering has not been subtracted out) and Fig. 5 shows the same data on a Log/Log plot.

4. DISCUSSION

4a. The dynamic structure factor

The most striking feature of the dynamic structure factor of myoglobin is the peak centered at 25 cm^{-1} observed at low temperatures (Fig. 1). Because in $S(q, \omega)$ modes are weighted by their amplitudes (see Eq. 2), the occurrence of the peak tells us that the dominant mean square vibrational displacements occur in myoglobin with a frequency of ~25 cm^{-1}. Similar low frequency peaks have been identified in several proteins by Raman spectroscopy at room temperature (19–21). Brown et al. found that the Raman peak at 29 cm^{-1} in chymotrypsin disappears upon SDS denaturation showing its sensitivity to protein secondary or tertiary structure and Genzel et al. found that the Raman peak at 25 cm^{-1} in crystalline lysozyme disappears upon dissolving the crystals. Chou has proposed that these modes correspond to accordion-like modes of α-helices and has made specific predictions for their frequencies (generally in the range 20–30 cm^{-1}) in a variety of proteins (22, 23). He has applied similar arguments to the breathing modes of β-sheets and barrels (24). To test this hypothesis we have made measurements of the dynamic structure factor of both acid and heat denatured myoglobin (results not shown). We find that the 25 cm^{-1} peak persists but with a slightly different shape. This suggests that the peak is not linked to internal deformations of secondary structure elements (in the case of myoglobin, α-helices), but to modes involving cross-chain interactions e.g., relative motions of α-helices. The interactions responsible for these modes will persist in a denatured molecule and hence would explain why the spectrum is only slightly modified.

4b. The vibrational frequency distribution of myoglobin

The frequency distributions derived at 100 and 180 K (see Fig. 4), where there is no quasielastic scattering, are very nearly superimposable below ~100 cm^{-1}. In other words, the variation with temperature of the inelastic scattering from myoglobin up to 180 K is consistent with that expected from a harmonic system and implies that the low frequency dynamics of myoglobin can be described by means of a distribution of underdamped vibrational modes. This is also consistent with the observed linear dependence on temperature (below ~ 180 K) of the atomic mean-square displacements both by neutrons (8) and by Mössbauer spectroscopy (1), again as expected for a quasi-harmonic system. In fact, Fig. 4 shows that the frequency distribution changes little in form right up to 350 K; the increasing enhancement at low frequencies above 180 K is due to the quasielastic scattering which has not been subtracted out. Systematic differences occur above 100 cm^{-1}, although it is possible that these are due to the neglect of multiphonon effects which enhance the scattering at high temperature and high q (i.e., at high angle and high ω in a time-of-flight measurement). Also it may be that the effective Debye-Waller factor is not the same at higher frequencies where the modes are more localized and the different Debye-Waller factors of different atoms become important.

Fig. 5 shows the myoglobin frequency distribution replotted on a log/log scale. This shows that at very low frequencies (below 20 cm^{-1}) the distribution is Debye-like, i.e., $G(\omega) \propto \omega^2$ as expected of a quasiharmonic continuum. However, there is a significant enhancement above the Debye form centered at 25 cm^{-1} (corresponding to the marked low frequency peak in the structure factor shown in Fig. 1), whereas above 40 cm^{-1} there is a deficit of modes. It should be stressed that although the enhancement in numbers of modes at 25 cm^{-1} is not very striking, the real physical significance of modes of this frequency is evident from the corresponding peak in $S_{inc}(q, w)$ as mentioned above in section 4a.

We now discuss the origin of the form of the vibrational density of states of myoglobin, firstly from the point of view of general theories of amorphous systems and secondly in comparison with detailed atomic models of protein dynamics which use empirical potential energy functions. In this respect we point out that other globular proteins that we have measured (lysozyme, BPTI, concanavalin A) all show spectral features similar to those of myoglobin suggesting that general features of protein structure (e.g., packing density, intramolecular force constants) should be sufficient to explain the form of the density of states.

The frequency distribution of amorphous diglycidyl ether of bisphenol A (DGEBA, the monomer from which most epoxy resins are made) (25) shows a cross-over from Debye behavior, $g(\omega) \propto \omega^2$, to a much weaker frequency dependence at a frequency corresponding to a length scale of ~ 30 Å. In the crystalline material the Debye behavior is maintained over a much larger frequency range. Similar anomalies are found in glassy systems (26). Alexander and Orbach (27, 28) have proposed that these results can be explained by a change in geometry from Euclidean at a large length scale ($r \gg \zeta$) to a fractal geometry at short length scales ($a < r < \zeta$), where a is the atomic spacing. One can associate the characteristic length ζ with a cross-over frequency ω_c. The high frequency vibrations have been termed fractions (27). Thus, fraction frequencies are $> \omega_c$ and phonon frequencies are $< \omega_c$. It was shown (29) that the density of states should follow $g(\omega) \propto \omega^{d-1}$ in the fractal regime. d is the spectral dimension of the fractal structure. For the cross-over region a scaling analysis (29) suggests an enhancement of $g(\omega)$ above the Debye behavior in the vincinity of ω_c.

Fig. 5 shows that the frequency distribution of myoglobin (i.e., that derived at 180 K or below) has approximately the form predicted for fractal systems with $\omega_c \sim 25$ cm^{-1}. Assuming a sound velocity of 3,000 m/s (30, 31) this frequency corresponds to a length scale of 40 Å, approximately the size of the myoglobin molecule. Thus, there is about one decade available for the evolution of the lower dimensional power law ($a \sim 4$ Å $- \zeta \sim 40$ Å). Although there is evidence from electron-spin relaxation that proteins do exhibit fractal-like spectral properties (32) (see below) there is no structural basis for self-similarity in proteins. However, these features in the frequency distribution may arise from other causes (33). An effective-medium approximation which emphasizes the low cross-chain hydrogen-bond connectivity in alpha-helical proteins has been used to show that in, for instance, myoglobin, the frequency distribution should vary as $\omega^{0.6}$ ($d = 1.6$) at low frequencies (34). In a different application of the effective medium approximation aimed at a description of phonons in glasses, it has recently been shown that characterizing the amorphous (disordered) nature of the system by a distribution of coupling constants can lead to an anomaly in $g(\omega)$ corresponding to a cross-over from low frequency free wave propagation to a high frequency strongly damped regime (35), without invoking fractal topology. It seems likely that generalizations of these latter theories of amorphous materials will eventually lead to a quantitative explanation of the density of states of myoglobin and other globular proteins.

An alternative approach to low frequency modes in proteins is based on computer simulation of protein dynamics using empirical force-fields and detailed struc-

tural models derived by x-ray crystallography (36). Molecular dynamics simulations give trajectories of each atom for periods up to 100's of picoseconds (nowadays usually in the presence of solvent molecules), whereas normal mode analysis makes the harmonic approximation assuming that it will be valid for small amplitude vibrations about a well-defined minimum energy configuration. Because these models include in principle all the effects specific to proteins mentioned above, they should be capable of reproducing observed spectra. However it remains open to question whether the potential energy functions are sufficiently accurate, whether the harmonic model is ever applicable, and whether from a molecular dynamics simulation of a single protein, it is possible to derive accurate ensemble average properties. In a recent comparison of the observed frequency distribution at 290 K of BPTI with various normal mode analyses of the protein (9, 10, 13, 14), it was noted that, even after allowing for the instrumental resolution function, the observed spectrum is always smoother than the calculated spectra, which predicted considerable structure in the density of vibrational modes (arising not from single modes, but a clustering of modes). The most likely explanation of this is damping effects due to anharmonicity and friction. In this paper we have shown that the density of states of myoglobin (and indeed BPTI) remains smooth down to low temperatures and behaves as expected for a quasiharmonic system. Unfortunately there is no published normal mode analysis of myoglobin yet. However, in view of the concept of conformational substates in proteins mentioned in the Introduction, it seems plausible that even at low temperatures there is no one well-defined structure about which vibrations occur and this will inevitably lead to a smooth spectrum. Some evidence for this comes from preliminary analysis of molecular dynamics simulations of myoglobin performed at 300 and 80 K (14). Incoherent inelastic neutron spectra calculated directly from these simulations show remarkable qualitative similarity with the differences observed experimentally as a function of temperature, i.e., a resolved inelastic peak in $S_{inc}(q, \omega)$ in the range 18–25 cm^{-1} is found from the 80 K simulation, whereas at 300 K the calculated spectrum is broad and monotonically decreasing. Furthermore, three separate simulations at 80 K, which appear to sample different regions of conformational space, give slightly different positions for the resolved inelastic peak, the average result being closer to the observed spectrum.

In summary, simplified theories of vibrations in amorphous systems may be sufficient to explain the form of the density of states measured in globular proteins. Such models may also remove the problem of separation of inter- and intramolecular modes in, for instance, a protein powder or crystal. However, detailed calculations using

empirical potential functions, particularly at a number of temperatures, may yield more insight in to the specific dynamics of proteins.

4c. Electron-spin relaxation

The electron-spin relaxation rate $(1/T_1)$ due to two-phonon (Raman) processes is given by (32):

$$\frac{1}{T_1} = \int_0^\infty \frac{\omega^4 [g(\omega)]^2 \exp{(\hbar\omega/k_B T)}}{[\exp{(\hbar\omega/k_B T)} - 1]^2} \, d\omega, \qquad (7)$$

where $g(\omega)$ is the vibrational density of states. For a system of dimension d, $g(\omega)$ is proportional to ω^{d-1} so that $1/T_1$ varies as T^{5+2d} (i.e., a normal Debye solid with $g(\omega) \propto \omega^2$ gives $1/T_1$ varying as T^9). It has been found (32, 37) that for ferric iron containing heme and nonheme proteins the temperature dependence of the Raman rate measured on frozen solutions between 4 and 20 K varies between $T^{5.7}$ (ferrodoxin) and $T^{6.3}$ (myoglobin). These anomalously low exponents appear to imply effective dimensionalities for protein vibrations in the range 1.35–1.65, respectively. An attempt has been made to relate these observations to a fractal description of protein structure (37), although the significance of the derived correlation is unclear. As mentioned above, an alternative explanation based on an effective medium treatment of the anisotropy of force constants in proteins has been proposed (34).

Having measured the (amplitude-weighted) vibrational density of states of a hydrated myoglobin powder by inelastic neutron scattering we can immediately use Eq. 7 to calculate the corresponding Raman relaxation rate and the result is plotted on a log/log scale in Fig. 6. This shows that below ~5 K, a Debye-like T^9 behavior is expected but that above this temperature there is a cross-over to a lower power law. The reason for this cross-over is evident from the form of the density of states plotted in Fig. 4. We do not think it useful to quote a value for the apparent fractal dimensionality of myoglobin derived from this data, firstly because there appears not to be a single power law and secondly because we have measured the density of states directly and do not need to deduce its form from an integrated property. However, it is clear that the form of the Raman relaxation rate for myoglobin predicted by the neutron results disagrees with the striking $T^{6.3}$ (and absence of T^9) behavior observed by electron-spin relaxation (32). This may be due to the difference in the nature of the samples (hydrated powder for neutrons, frozen solutions for ESR); differences in the density of states between 4–20 K (ESR) and 100–180 K (neutrons); or incorrect weighting by the neutrons of the phonons responsible for the Raman relaxation. On the other hand, Fig. 6 shows more similarity with the ESR
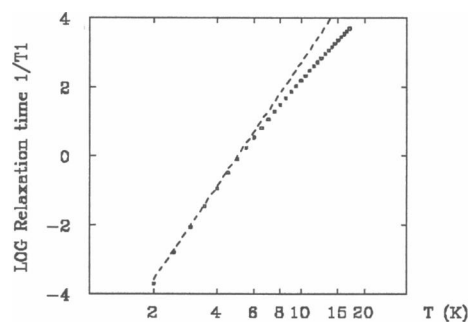

FIGURE 6   Log/log plot of the Raman relaxation rate $1/T_1$ (arbitary scale) calculated from the amplitude-weighted vibrational frequency distribution of myoglobin at 180 K (*circles*). The dashed straight line has slope 9 (Debye behavior).

result for myoglobin azide in a solvent of 50% glycerol/water (37). Here a transition from T^9 to $T^{6.22}$ behavior is observed near 6 K. This is attributed to a cross-over from solvent (Debye) to protein (fractal) vibrational modes when the phonon wavelength becomes smaller than the size of the protein molecule. Whether or not this is the correct explanation, it does raise the difficulty of distinguishing between inter- and intramolecular modes in concentrated or frozen protein systems.

4d. Separation of quasielastic and inelastic scattering

We can use the results of section 3 to obtain the form of the quasielastic scattering for temperatures above 180 K. From Eqs. 4 and 6 we find:

$$S_{qel}(q, \omega, T) = S(q, \omega, T)$$
$$- S(q, \omega, T_0) \frac{e^{-q^2 U_{vib}(T)}(e^{\hbar\omega/k_B T_0} - 1)}{e^{-q^2 U_{vib}(T_0)}(e^{\hbar\omega/k_B T} - 1)}. \qquad (8)$$

The results are shown in Fig. 7. The integrated quasielastic intensity increases with temperature with dependence $\exp(-\Delta E/RT)$, where $\Delta E = 13 \pm 1$ kJ/mol. In a previous paper (8), a more detailed interpretation of the elastic and quasielastic scattering is presented in terms of a model of hydrogen motion between sites of energy asymmetry ΔE. There it is shown that this additional motion excited above 180 K leads to a sharp extra increase in the mean-square atomic displacements. Fourier transform of the curves in Fig. 7 with simultaneous deconvolution of the instrumental resolution function shows that the corresponding time-correlation function have a fast component ($\tau \sim 0.3$ ps) and a slower component ($\tau \sim$ several ps)(8).

The crucial assumption in this analysis is that the vibrational mode frequencies are temperature indepen-
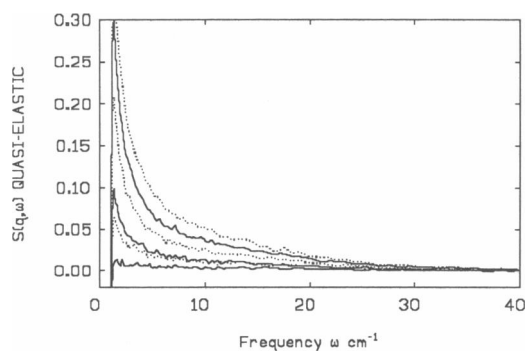
FIGURE 7 Quasielastic spectra for temperatures above 180 K obtained by subtraction of the scaled inelastic scattering at 180 K for a fixed scattering angle of 108.3°. The temperatures are 220 K (*bottom curve*), 250 K, 270 K, 300 K, 320 K, and 350 K (*top curve*).

dent. This appears to be the case above 4 meV (Fig. 2), but it cannot be ruled out that some of what we call quasielastic scattering arises from low frequency mode softening due to frictional or other anharmonic effects. However, it is striking that the form of the quasielastic scattering (Fig. 7) is virtually temperature independent (the amplitude varying with dependence exp $[-\Delta E/RT]$, see above). This is more easily understood in terms of a well-defined dynamic process (8), rather than mode softening which would be expected to lead to a spectral form changing more smoothly with temperature.

5. CONCLUSION

Inelastic neutron scattering data on a D_2O-hydrated powder of myoglobin as a function of temperature have been used to show that below 180 K myoglobin behaves as a quasiharmonic material characterized by an almost temperature independent vibrational frequency distribution. The latter is a smooth function similar in form to a variety of other amorphous and glassy systems. Above 180 K there is an onset of quasielastic scattering which can be separated from the vibrational motion and has been analyzed more fully elsewhere (8; 38; Doster, W., S. Cusack, and W. Petry, manuscript submitted for publication). The results presented here are not unique to myoglobin; qualitatively similar behavior is found for hydrated powders of lysozyme and BPTI, although the position of the peak in the structure factor varies slightly (unpublished results). This suggests that the dynamical behavior of globular proteins at the level of detail observed here is not very sensitive to secondary structure.

REFERENCES

1. Parak, F., E. W. Knapp, and D. Kucheida. 1982. Protein dynamics: Mössbauer spectroscopy on deoxymyoglobin crystals. *J. Mol. Biol.* 161:177–194.

2. Parak, F., J. Heidemeier, and G. U. Nienhaus. 1988. Protein structural dynamics as determined by Mössbauer spectroscopy. *Hyperfine Interactions.* 40:147–158.

3. Austin, R. H., K. W. Beeson, L. Eisenstein, H. Frauenfelder, and C. Gunsalus. 1975. Dynamics of ligand binding to myoglobin. *Biochemistry.* 14:5355–5373.

4. Ansari, A., J. Berendson, S. F. Bowne, H. Frauenfelder, I. E. T. Iben, T. B. Sauke, E. Shyamsunder, and R. D. Young. 1985. Protein states and proteinquakes. *PNAS* 82:5000–5004.

5. Parak, F., H. Hartmann, K. D. Aumann, H. Reuscher, G. Rennekamp, H. Bartunik, and W. Steigemann. 1987. Low temperature X-ray investigation of structural distributions in myoglobin. *Eur. Biophys. J.* 15:237–249.

6. Elber, R., and M. Karplus. 1987. Multiple conformational states of proteins: a molecular dynamics analysis of myoglobin. *Science (Wash. DC).* 235:318–321.

7. Doster, W., A. Bachleitner, R. Dunau, M. Hiebl, and E. Lüscher. 1986. Thermal properties of water in myoglobin crystals and solutions at subzero temperatures. *Biophys. J.* 50:213–219.

8. Doster, W., S. Cusack, and W. Petry. 1989. Dynamical transition of myoglobin revealed by inelastic neutron scattering. *Nature.* 337:754–756.

9. Cusack, S. 1989. Low frequency dynamics of proteins studied by inelastic neutron scattering. *In* The Enzyme Catalysis Process: Energetics, Mechanism and Dynamics. *NATO ASI (Adv. Sci. Inst.) Ser. A Life Sci.* 178:103–122.

10. Cusack, S. 1989. Low frequency dynamics of proteins: comparison of inelastic neutron scattering results with theory. *Chem. Sci.* 29A:103–107.

11. Lovesey, S. W. 1984. Theory of neutron scattering from condensed matter. Clarendon Press, Oxford. 1:

12. Bee, M. 1988. Applications of quasielastic neutron scattering to solid-stated chemistry, biology, and material science. Adam Hilger, London.

13. Cusack, S., J. Smith, J. Finney, B. Tidor, and M. Karplus. 1988. Inelastic neutron scattering analysis of picosecond internal protein dynamics: comparison of harmonic theory with experiment. *J. Mol. Biol.* 202:903–908.

14. Smith, J., K. Kuczera, B. Tidor, M. Karplus, W. Doster, and S. Cusack. 1989. Internal dynamics of globular proteins: comparison of neutron scattering measurements and theoretical models. *Physica.* B156–157:437–443.

15. Guide to neutron research facilities at the Institut Laue-Langevin. 1988. ILL, Grenoble, France.

16. Smith, J., S. Cusack, U. Pezzeca, B. R. Brooks, and M. Karplus. 1986. Inelastic neutron scattering analysis of low-frequency motion in proteins: a normal mode study of the bovine pancreatic trypsin inhibitor. *J. Chem. Phys.* 85:3636–3654.

17. Sears, V. F. 1975. Slow-neutron mutliple scattering. *Adv. Phys.* 24:1–45.

18. Frick, B., D. Richter, W. Petry, and U. Buchenau. 1988. Study of the glass transition order parameter in amorphous polybutadiene by incoherent neutron scattering. *Z. Phys.* B70:1–3.

19. Brown, K. G., S. C. Erfurth, E. W. Small, and W. L. Peticolas. 1974. Conformationally dependent low frequency motions of proteins by laser Raman spectroscopy. *PNAS* 69:1467–1469.

20. Genzel, L., F. Keilmann, T. P. Martin, G. Winterling, Y. Yacoby, and M. W. Makinen. 1976. Low frequency Raman spectra of lysozyme. *Bioploymers.* 15:219–225.

21. Painter, P. C., L. E. Mosher, and C. Rhoads. 1982. Low frequency modes in the Raman spectra of proteins. *Biopolymers.* 21:1469–1472.

22. Chou, K-C. 1984. Biological functions of low-frequency vibrations (phonons): III. Helical structures and microenvironment. *Biophys. J.* 45:881–890.

23. Chou, K-C. 1984. Biological functions of low-frequency vibrations (phonons): 4. Resonance effects and allosteric transition. *Biophys. Chem.* 20:61–71.

24. Chou, K-C. 1985. Low-frequency motions in protein molecules: β-sheet and β-barrel. *Biophys. J.* 48:289–297.

25. Dianoux, A. J., J. N. Page, and H. M. Rosenberg. 1987. Inelastic neutron scattering in the amorphous and crystalline state: the phonon-fracton density of states. *Phys. Rev. Lett.* 58:886–888.

26. Buchenau, U., M. Prager, N. Nücker, A. J. Dianoux, N. Ahmad, and W. A. Phillips. 1986. Low frequency modes in vitreous silica. *Phys. Rev.* B34:5665–5670.

27. Alexander, S., and R. Orbach. 1982. Density of states on fractals: "fractions". *J. Phys. Lett.* 43:L625–L631.

28. Orbach, R. 1986. Dynamics of fractal networks. *Science (Wash. DC).* 231:814–819.

29. Aharony, A., S. Alexander, O. Entin-Wohlman, and R. Orbach.

1985. Scaling approach to phonon-fracton crossover. *Phys. Rev.* B31:2565–2567.

30. Cusack, S., and S. Lees. 1984. Variation of longitudinal acoustic velocity at gigahertz frequencies with water content in rat-tail tendon fibres. *Biopolymers.* 23:337–351.

31. Randall, J. T., and J. M. Vaughan. 1979. Brillouin scattering in systems of biological interest. *Phil. Trans. Roy. Soc. Lond.* A293:341–348.

32. Allen, J. P., J. T. Colvin, D. G. Stinson, C. P. Flynn, and H. J. Stapleton. 1982. Protein conformation from electron spin relaxation data. *Biophys. J.* 38:299–310.

33. Krumhansl, J. A. 1986. Vibrational anomalies are not generally due to fractal geometry: comments on proteins. *Phys. Rev. Lett.* 56:2696–2699.

34. Elber, R., and M. Karplus. 1986. Low-frequency modes in proteins: use of effective-medium approximation to interpret the fractal dimension observed in electron-spin relaxation measurements. *Phys. Rev. Lett.* 56:394–397.

35. Schirmacher, W., and M. Wagener. 1989. Phonons in glasses. *In* Dynamics of Disordered Materials. D. Richter, A. J. Dianoux, W. Petry, and J. Teixeira, editors. Springer-Verlag, Berlin. 37:231–234.

36. McCammon, J. A., and S. C. Harvey. 1987. Dynamics of proteins and nucleic acids. Cambridge University Press, Cambridge.

37. Colvin, J. T., and H. J. Stapleton. 1985. Fractal and spectral dimensions of biopolymer chains: solvent studies of electron spin relaxation rates in myoglobin azide. *J. Chem. Phys.* 82:4699–4706.

38. Doster, W., S. Cusack, and W. Petry. 1989. Scaling properties of fast motions in a globular protein. *In* Dynamics of Disordered Materials. D. Richter, A. J. Dianoux, W. Petry, and J. Teixeira, editors. Springer-Verlag, Berlin. 37:120–123.